JOURNAL OF PROPULSION AND POWER
Vol. 22, No. 3, May–June 2006

Effects of Vaneless Diffuser Geometries on Rotating Stall

Kamorudeen B. Abidogun*
Saudi Basic Industries Corporation, Jubail Industrial City, 31961 Saudi Arabia

Detailed experimental investigation was carried out primarily to document the effects of vaneless diffuser diameter and width ratios on the fundamental characteristics of flow perturbation in the vaneless diffuser of a centrifugal blower. A benchmark set of experimental data is provided to aid numerical investigation of instabilities in the vaneless diffuser flow field in particular and the entire compression system in general. The synchronous speed was also varied to study the effect of shaft speed on stall features. The current data showed that a decrease of the diffuser width, at constant impeller angular speed, resulted in an increase of the critical flow coefficient. The data further revealed that an increase in the diffuser diameter ratio resulted in an increase in the frequency of rotating stall. Unlike diffuser diameter ratio, variation of the diffuser width ratio does not have an appreciable effect on the frequency of rotating stall.

Nomenclature

b	=	diffuser width, m
C_p	=	pressure coefficient, $(P_o - P_{\text{imp}})/(\rho V_{\text{imp}}^2/2)$
D	=	diffuser diameter, m
f_p	=	frequency of stall cells, Hz
N	=	impeller speed, rpm
N_s	=	angular speed of stall cells, 60 f_p/n rpm
n	=	number of stall cells
P	=	fluctuating pressure, Pa
r	=	radial distance, m
V	=	mean velocity, m/s
V_{imp}	=	impeller tip speed, m/s
y	=	axial distance, m
ρ	=	density of air, kg/m^3
Φ	=	phase angle between dynamic pressure signals, deg
ϕ	=	flow coefficient, V_r/V_{imp}
φ	=	coherence factor

Subscripts

cr	=	critical condition
i	=	diffuser inlet
imp	=	associated with the impeller
o	=	diffuser outlet

Introduction

CENTRIFUGAL compressors are vital in many industrial applications, such as those typical of petrochemical, process, oil, and refrigeration and air conditioning industries. Flow downstream of a centrifugal compression system has received considerable attention in the past, as well as the present, because of its significant impact on machine efficiency and range of operation. For example, flow instabilities in centrifugal compressors could cause shaft vibrations, which usually lead to increased wear on the compressor bearings and reduce the performance of the compressor, particularly at low flow rates. Hence, efforts have been made by researchers to describe flow instabilities in centrifugal compressors, and they have sought ways to ensure that this instability is far removed from the compressor stable operating range, which is normally indicated on the system performance map of the compressor data sheet.

The effects of diffuser wall roughness on rotating stall in vaneless diffusers of centrifugal blowers has been studied.[1] In this study, the flow rate at rotating stall inception was decreased by 42% when a completely rough wall was positioned on the hub side of the diffuser wall. Flow instabilities associated with vaneless diffusers have been studied and characterized.[2–6] These studies were carried out in the form of theoretical analysis and experimental measurements. Experiments to determine the characteristics of oscillating flows in a centrifugal compression system with vaneless diffusers have been conducted.[7] The system was operated without a diffuser and with eight different diffuser configurations to determine the effects of diffuser diameter and width ratios on the unsteady behavior of the system. It was found that the critical flow coefficients, at which onset of oscillations was observed, increased as the diffuser width ratio was decreased, whereas it decreased as the diameter ratio was increased. Thus, the critical flow was dependent on diffuser diameter and width ratios. The rotational speeds of the oscillation patterns had a strong dependence on the diffuser diameter ratio and a weak dependence on the width ratio.

This paper documents the effects of vaneless diffuser diameter and width ratios on the fundamental characteristics of flow perturbations in the vaneless diffuser of a centrifugal blower. There are little data available in the open literature on this subject. Therefore, more data are necessary to augment the existing data. To achieve these objectives, detailed measurements were taken in the vaneless diffusers of a centrifugal blower, which were analyzed to document the effect of diffuser width and diameter ratios on diffuser flow instabilities.

Experimental Setup and Instrumentation

The experimental rig used for this experiment was designed and built in-house and is shown in Fig. 1. It consists of a centrifugal compressor air intake, an impeller housing, an actual impeller, and a vaneless diffuser. A moving, streamlined, axisymmetric plug through the air intake controls the mass flow through the impeller. The impeller used for delivering the flow has 28 blades aligned in the radial direction. At the exit, it has a tip height of 12.6 mm. With an inlet diameter of 85 mm, the impeller measures 228 mm diameter at its outlet. It is driven by a 2.5 hp, variable speed, electric motor at a rotational speed N of 2000 rpm (blade passing frequency of 933 Hz (55980 CPM)). This produced a Reynolds number of about 3.6×10^5, based on the impeller tip speed, 23.9 m/s and outlet diameter. The machine Mach number based on the inlet flow condition (atmospheric) is 0.07. Shaft speed was also varied to study the effect of speed on stall features. The vaneless diffuser has parallel walls with a width ratio b/D_i of 0.035 and a diameter ratio D_o/D_i of 1.5. Provision was made for extending the diffuser width and diameter ratios to 0.055 and 2.0, respectively.

Received 8 September 2004; revision received 7 May 2005; accepted for publication 7 September 2005.

*Senior Rotating Machinery Engineer, Engineering and Project Management, Box 11425; abidogunkb@sabic.com.

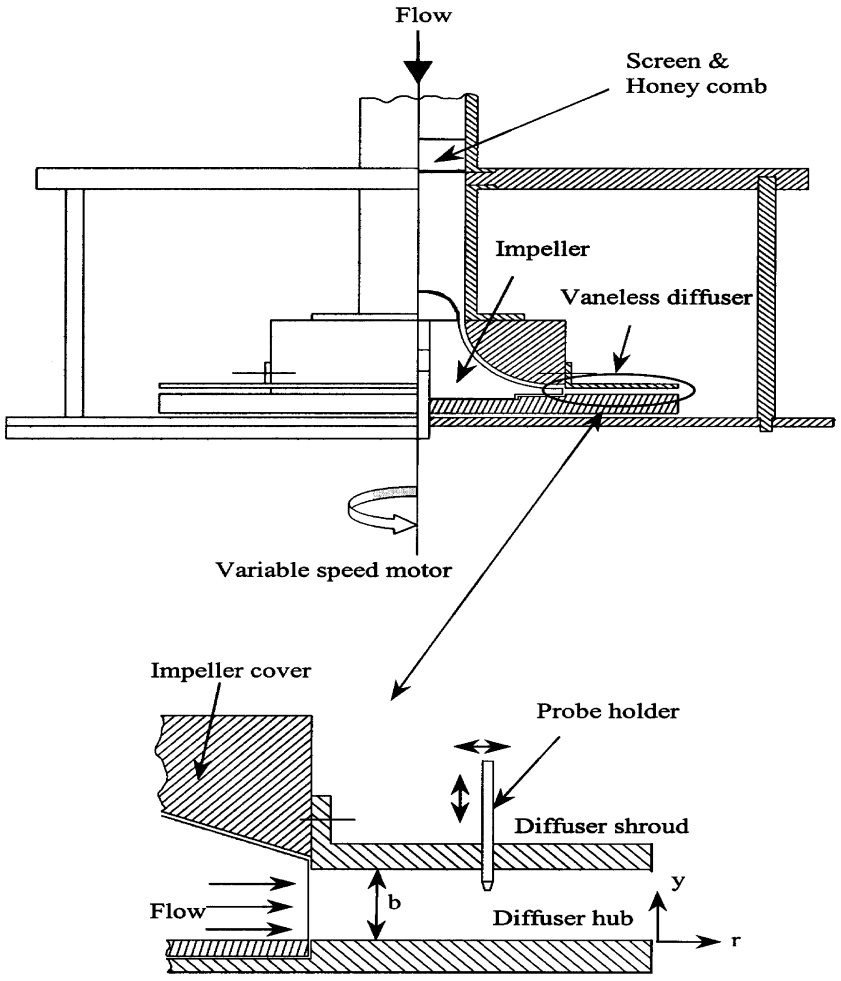

Fig. 1 Schematic of test section.

An x-wire miniature probe was used to record the instantaneous radial and circumferential velocities at the entrance of the diffuser and halfway between the diffuser hub and shroud. The data from these measurements were used to calculate the flow coefficient. The x-wire probe was calibrated using King's law calibration formula. The unsteady flow characteristics were measured using dynamic PCB Piezotronics pressure transducers (Model 112A22). The natural frequency of the pressure sensors is 300 kHz. They were designed for low-pressure, high-resolution applications, which make them suitable for the current study. The transducers were flush mounted on the diffuser shroud wall to determine the stall cells characteristics. Details of the measurement procedures have been reported.[8,9] The accuracy of the results was checked by numerically integrating the radial velocity component to obtain the mass flow rate at each of the measurement stations. When compared to the throughput at the inlet of the impeller, the maximum error recorded was less than 7%.

Experimental Results and Discussion

Rotating Stall Inception and Propagation

The method employed for the detection of rotating stall was similar to the one employed in Ref. 10 but with more detailed analysis. The pressure traces from the dynamic pressure transducers at locations 1–6 (Fig. 2), which were low-pass filtered at 100 Hz to eliminate frequencies other than the rotating stall's, were recorded and digitized for later analysis. In particular, the number of rotating stall cells and their speed of rotation relative to the impeller speed were determined from the outputs of the pressure transducers at locations 2 and 4.

The time series of the output signal from the pressure transducers at pre- and poststall inception, for $b/D_i = 0.055$ and $D_o/D_i = 1.5$, are shown in Figs. 3a–3d. Figure 3a is the pressure signal captured just before stall inception at $\phi = 0.198$ and characterizes all pressure signals recorded before stall inception (from $\phi = 0.479$ to 0.198). The critical flow coefficient ϕ_{cr} is 0.148, which corresponds to Fig. 3b. This flow coefficient corresponds to the onset of flow perturbations. Flow instability persisted with further reduction of throughput to $\phi = 0.041$ as indicated in Figs. 3b–3d. Note that the critical flow coefficient was measured at diffuser inlet, $r/r_i = 1.05$, and at half-channel width. The critical flow angle measured at the same location, and from the diffuser radial direction, is about 81 deg. This location is a close approximation of the conditions at the impeller tip because the tangential component of the velocity is approximately equal to the impeller tip speed.

Figures 4a–4d show the spectra of pressure fluctuations in Figs. 3a–3d. The distinct spike in Fig. 4a occurring at a frequency of 67 Hz is two times the synchronous frequency of 33.33 Hz. This is an indication of a possible small shaft misalignment. It is not of any concern because the amplitude is small compared to the amplitude of the dominating stall frequency as throughput was reduced further.

At the onset of rotating stall, which corresponds to Fig. 4b, both the power spectral density [(input unit)^2/hertz] (PSD) and cross-spectral density [(input unit^2)/hertz] (CSD) plots show the emerging stall cells at virtually the same strength level. This is a confirmation that the effect of the perturbation patterns was felt uniformly at both pressure sensors locations, 45 deg apart circumferentially. The CSD is very useful in differentiating stall cells

Table 1 Comparison of stall cells features

Author	ϕ	f_p, HZ	CSD	φ	Φ	n	N_s/N
Present work, $D_o/D_i = 1.5$,	0.148	13.4	37.7	1.00	−53.2	1	0.403
$b/D_i = 0.055$, $N = 2000$ rpm		26.9	21.3	1.00	−88.9	2	0.403
		40.3	3.2	0.97	−130.2	3	0.403
	0.131	13.4	49.9	1.00	−51.6	1	0.403
		26.9	15.1	1.00	−87.8	2	0.403
		53.7	1.1	0.98	−178.9	4	0.403
	0.106	13.4	58.7	1.00	−51.0	1	0.403
		26.9	6.4	0.99	−83.4	2	0.403
		40.3	1.9	0.97	−138.9	3	0.403
		53.7	2.6	0.95	−163.3	4	0.403
	0.061	12.2	56.3	1.00	−48.3	1	0.366
		25.6	15.3	0.98	−86.5	2	0.385
	0.041	12.2	59.7	0.99	−51.7	1	0.366
		25.6	15.3	0.98	−86.5	2	0.385
Abdelhamid and Bertrand (Ref. 16),		27.0				1	0.324
$D_o/D_i = 1.55$,		54.0				2	0.324
$b/D_i = 0.054$, $N = 5000$ rpm							
Otugen et al.,[10] $D_o/D_i = 1.5$,		7.3				1	0.332
$b/D_i = 0.056$, $N =$ 1320 rpm		14.5				2	0.330
Mizuki and Oosawa[17] (1992), $D_o/D_i = 1.59$,		55.0				1	0.330
$b/D_i = 0.071$, $N = 10{,}000$ rpm							
Watanabe et al.,[2] $D_o/D_i = 2.25$,		10.0				1	0.209
$b/D_i = 0.066$, $N = 2865$ rpm		14.5				2	0.152

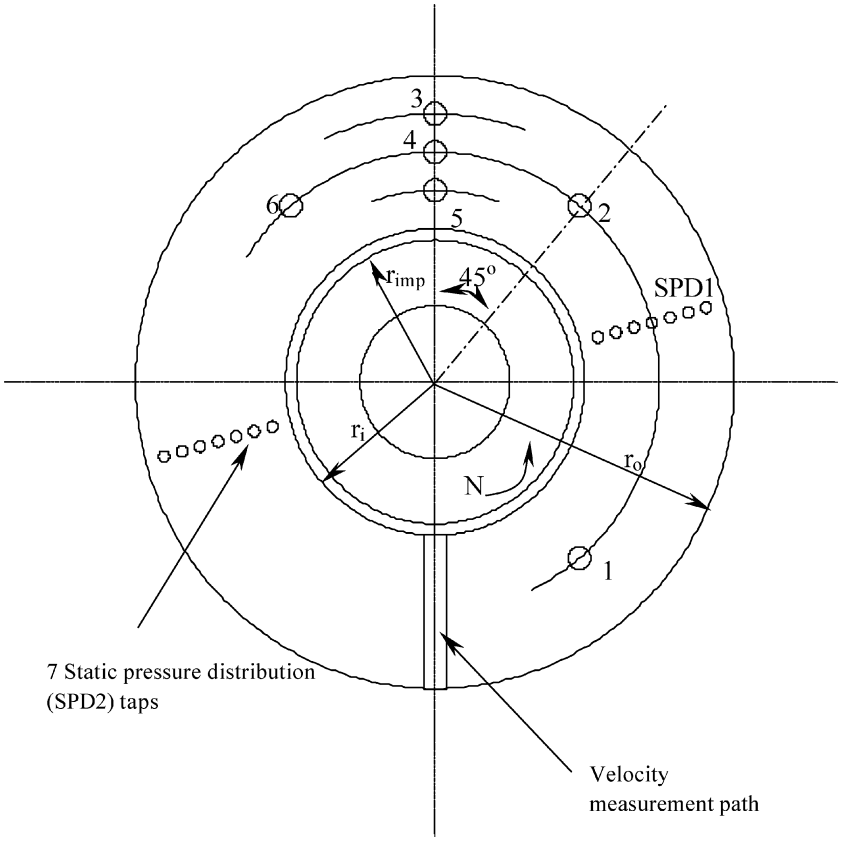

Fig. 2 Dynamic pressure transducer locations (1–6) on shroud wall.

from other local excitations. For example, PSD in Fig. 4b shows a strong excitation at 67 Hz on pressure probe 2 but inconspicuous excitation on pressure probe 1. The incoherence of the 67 Hz structure between both pressure probes locations, strengthwise, is clearly obvious in the CSD plot. (Note that 67 Hz has insignificant amplitude).

After stall inception, flow perturbation persisted as the flow coefficient was reduced further. Table 1 shows stall cell features measured at impeller speed of 2000 rpm in comparison with results from other investigators. The negative phase angle between the two pressure transducers indicate that the stall cells were propagating in the same direction as the impeller.[11] That is, the probe at location 2 in Fig. 2 "sees" the stall cell before the probe at location 4. The primary stall cell is 13.4 Hz at the onset of rotating stall, $\phi_{cr} = 0.148$. It has second, third, and fourth harmonics, at $\phi > 0.061$, of 26.9, 40.3, and 53.7 Hz, respectively. Thus, this range of flow coefficient features, essentially, one stall cell propagating at a frequency of 13.4 Hz, with its three harmonics, propagating at an angular speed of about 40% of

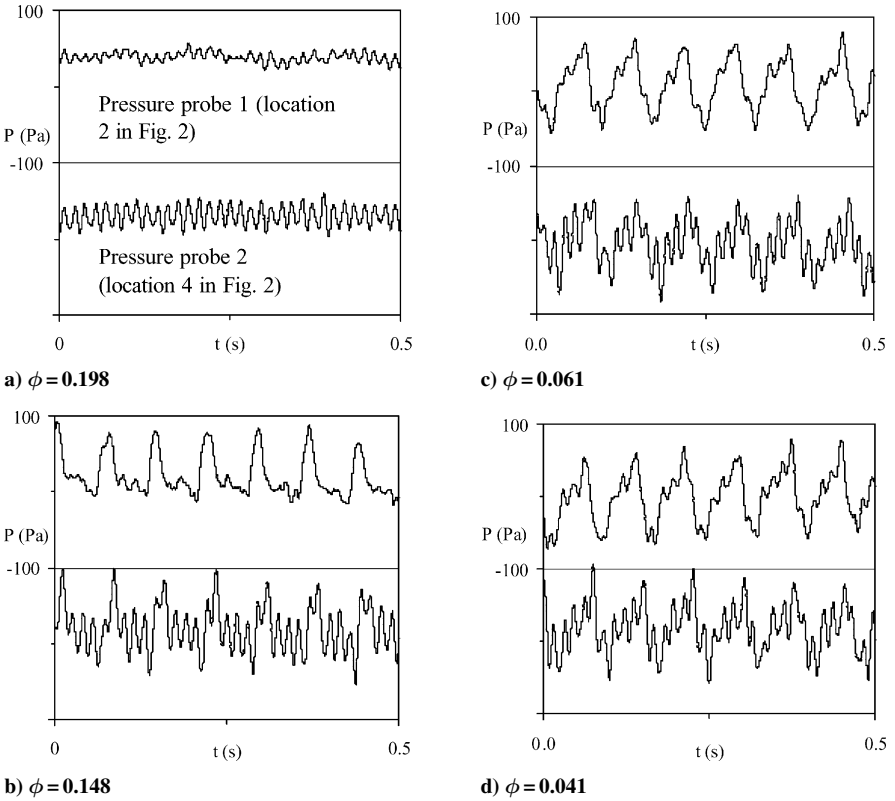

a) $\phi = 0.198$ **c)** $\phi = 0.061$

b) $\phi = 0.148$ **d)** $\phi = 0.041$

Fig. 3 Pressure signal of stall development, $b/D_i = 0.055$ and $D_o/D_i = 1.5$.

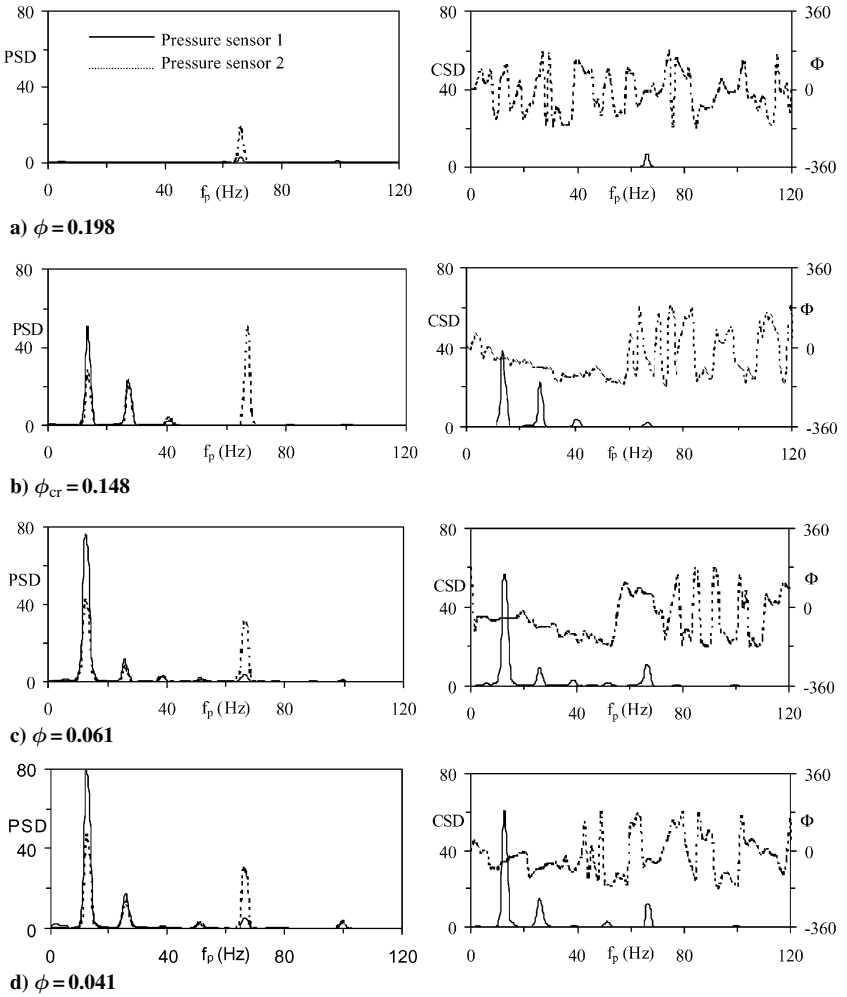

a) $\phi = 0.198$

b) $\phi_{cr} = 0.148$

c) $\phi = 0.061$

d) $\phi = 0.041$

Fig. 4 Spectra of pressure signal of stall development, $b/D_i = 0.055$ and $D_o/D_i = 1.5$.

the synchronous speed. Note that the three harmonics, though highly coherent as shown in Table 1, have very small amplitudes (CSD values in Table 1) when compared to the amplitude of the fundamental frequency. At much lower flow coefficients, the angular speed of the primary stall cell was about one-third of the synchronous speed, for example, at $\phi = 0.061$. These results are in good agreement with the experimental results in Ref. 12, where stall cell angular speed of about one-third of the impeller angular speed was reported. The decrease of the stall cell frequency from 13.4 to 12.2 Hz at much lower flow rate may be an indication that stall cell frequency is influenced by throughput flow.[11]

Furthermore, the effect of Reynolds number, N, or b/D_i on N_s/N values is insignificant, whereas the effect of increasing D_o/D_i tends to decrease their values.[11] This is probably why the current values of N_s/N are slightly higher than those reported by other investigators who employed higher diameter ratios in their investigation, as shown in Table 1. As noted earlier, the speed of the rotating stall approaches one-third of the impeller synchronous speed as flow coefficient was reduced further. With larger diffuser diameter ratio, $D_o/D_i = 2.0$ and $b/D_i = 0.055$ as shown later in Table 2, stall cell speed is about 32% of impeller angular speed. This is a confirmation of the expected effect of diffuser diameter ratio on stall cell speed as described at the beginning of this paragraph.

Effects of Diffuser Geometries on Stall Inception

Diffuser Width Ratio

Figure 5 shows the variation of critical flow coefficient with the diffuser width ratio and diffuser diameter ratio. With diameter ratio of 2, the critical flow coefficients (measured at the diffuser inlet) are 0.256, 0.265, and 0.276 for width ratios 0.055, 0.046, and 0.035, respectively. That is, critical flow coefficient increases as the diffuser width ratio is decreased. In other words, increasing the diffuser width ratio results in an increase in the stability of the blower, if all other diffuser geometries are kept constant. Note that there are differences of opinion on the effect of diffuser width on the stability of the blower, with Jansen[13] predicting a stable blower with a decreasing diffuser width, whereas Senoo and Kinoshita[14] predict otherwise, as found in the present work.

Figure 6 shows the effect of diffuser width on measured static pressure coefficient against diffuser inlet flow coefficient. Although

Table 2 Effects of diffuser width ratio on stall cell characteristics, $D_o/D_i = 2$

b/D_i	N	f_p	PSD1	PSD2	CSD	φ	Φ	n	N_s/N
0.055	500	2.69	1.09	0.79	0.91	0.977	−48.7	1	0.322
0.055	500	5.37	0.11	0.16	0.12	0.869	−87.7	2	0.322
0.045	500	2.44	1.27	0.87	1.05	0.991	−48.0	1	0.293
0.045	500	5.13	0.38	0.10	0.18	0.934	−71.9	2	0.308
0.035	500	2.44	0.96	0.59	0.75	0.991	−48.9	1	0.293
0.035	500	4.88	0.24	0.11	0.16	0.879	−84.9	2	0.293
0.055	1000	5.37	7.80	7.00	7.38	0.997	−43.1	1	0.322
0.055	1000	10.50	0.44	0.41	0.42	0.968	−88.1	2	0.315
0.045	1000	5.13	12.63	8.81	10.54	0.998	−46.2	1	0.308
0.045	1000	10.25	0.65	0.49	0.56	0.997	−85.3	2	0.308
0.035	1000	4.88	8.42	6.58	7.42	0.995	−46.0	1	0.293
0.035	1000	9.77	0.62	0.56	0.58	0.988	−84.4	2	0.293
0.055	1500	8.06	27.91	29.52	28.70	1.000	−48.0	1	0.322
0.055	1500	16.11	1.74	1.51	1.62	0.998	−95.7	2	0.322
0.045	1500	7.81	37.36	33.59	35.40	0.999	−47.2	1	0.313
0.045	1500	15.63	2.19	2.10	2.14	0.999	−87.4	2	0.313
0.035	1500	7.32	22.51	19.14	20.74	0.999	−45.3	1	0.293
0.035	1500	14.89	1.66	1.55	1.60	0.995	−100.9	2	0.298
0.055	2000	10.74	65.37	64.52	64.93	1.000	−46.9	1	0.322
0.055	2000	21.48	3.58	4.06	3.81	0.998	−91.5	2	0.322
0.045	2000	10.25	66.97	63.08	64.98	1.000	−46.2	1	0.308
0.045	2000	20.75	3.91	0.62	1.53	0.974	−84.2	2	0.311
0.035	2000	10.01	56.60	50.71	53.50	0.997	−41.2	1	0.300
0.035	2000	19.78	2.02	2.28	2.12	0.973	−134.4	3	0.198

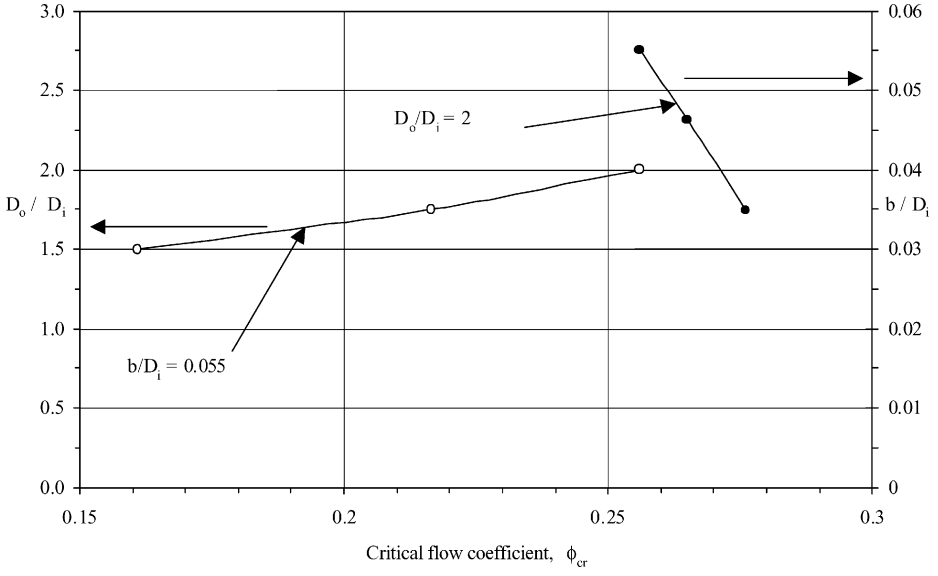

Fig. 5 Effects of diffuser geometries on stall inception.

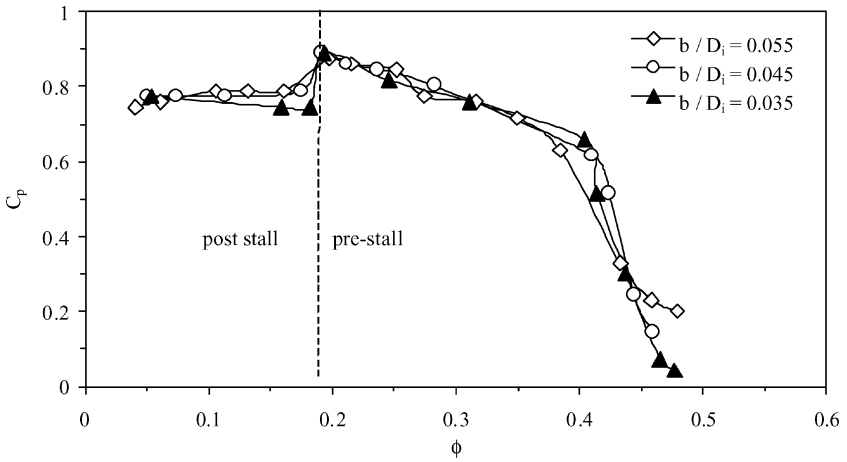

Fig. 6 Static pressure coefficient as a function of flow coefficient, $D_o/D_i = 1.5$.

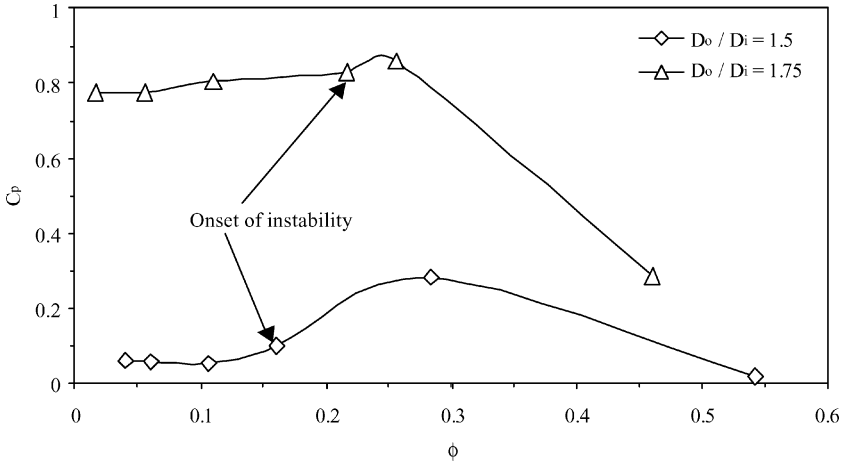

Fig. 7 Static pressure coefficient as function of flow coefficient, $b/D_i = 0.055$.

the trend of the critical flow coefficient is as described earlier, the dependence of the parameters plotted on diffuser width is not clearly marked. This probably explains why there are differences of opinion on this issue as discussed in the preceding paragraph.

Diffuser Diameter Ratio

For a fixed diffuser width, $b/D_i = 0.055$, the critical flow coefficients measured are 0.161, 0.217, and 0.256 for diameter ratios 1.5, 1.75, and 2.0, respectively. Hence, increasing the diffuser diameter ratio resulted in an increase of the critical flow coefficient (Fig. 5), suggesting a more stable flow at smaller diameter ratios. It is well established that the diffuser diameter ratio increase usually results in increasing the pressure at the diffuser exit. This is clearly shown in Fig. 7. Diffuser diameter ratio increase beyond 2 is usually not encouraged. Further pressure recovery not achievable with diffuser diameter ratio of 2 is usually done with the aid of a volute.[15]

Effects of Diffuser Geometries on Stall Characteristics

Diffuser Width Ratio

Table 2 shows the effect of diffuser width ratio on the characteristics of stall cells at a fixed diffuser diameter ratio of 2. The results show a slight decrease in the nondimensional speed of stall cells when the diffuser width ratio was decreased. For example, when the diffuser width ratio was decreased by 36.5%, only a decrease of 9.1% in the nondimensional angular speed was recorded for the single-lobe stall cell. The results in Ref. 16 showed an increase of about 10% in the nondimensional speed of the single-lobe stall cell when the diffuser width ratio was decreased by 40%.

Variations of the strength (CSD) of rotating stall cells with the diffuser width, at different shaft speeds, are shown in Fig. 8. Figure 8

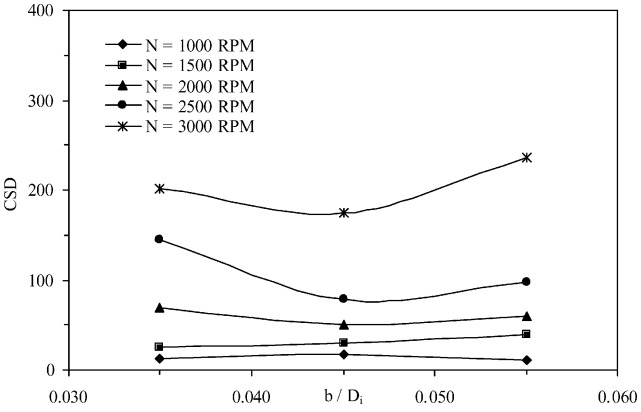

Fig. 8 Effects of diffuser width ratio on the strength of rotating stall cells, $D_o/D_i = 1.5$.

does not show any systematic dependence of stall strength on the diffuser width ratio, although the effect of shaft speed on CSD is expectedly noticeable: CSD increasing with speed at constant width ratio. For example, at shaft speeds of 2500 and 3000 rpm, the strength of stall cells decreases as the diffuser width ratio was increased from $b/D_i = 0.035$ to 0.045 and then increases with further increase of the diffuser width ratio. Thus, it is possible to claim that the strength of stall cells is independent of the diffuser width.

Figure 9 shows the variation of f_p, at different impeller angular speeds, as a function of diffuser width ratio. Figure 9 clearly confirms that f_p decreases as impeller angular speed was decreased, irrespective of the diffuser width. Furthermore, the frequency of pressure

Table 3 Effects of diffuser diameter ratio on stall cell characteristics, $b/D_i = 0.055$

D_o/D_i	N	f_p	PSD1	PSD2	CSD	φ	Φ	n	N_s/N
2	500	2.686	1.09	0.79	0.91	0.977	−48.7	1	0.322
2	500	5.371	0.11	0.16	0.12	0.869	−87.7	2	0.322
2	1000	5.371	7.80	7.00	7.38	0.997	−43.1	1	0.322
2	1000	10.498	0.44	0.41	0.42	0.968	−88.1	2	0.315
2	1500	8.057	27.91	29.52	28.70	1.000	−48.0	1	0.322
2	1500	16.113	1.74	1.51	1.62	0.998	−95.7	2	0.322
2	2000	10.742	65.37	64.52	64.93	1.000	−46.9	1	0.322
2	2000	21.484	3.58	4.06	3.81	0.998	−91.5	2	0.322
1.75	500	2.930	1.21	0.96	1.07	0.984	−47.9	1	0.352
1.75	500	5.859	0.30	0.19	0.22	0.882	−83.0	2	0.352
1.75	1000	5.859	9.91	6.51	8.03	0.999	−45.5	1	0.352
1.75	1000	11.963	1.60	0.80	1.12	0.994	−84.1	2	0.359
1.75	1500	9.033	16.70	21.53	18.94	0.998	−58.8	1	0.361
1.75	1500	18.311	8.45	4.43	6.11	0.999	−81.1	2	0.366
1.75	2000	12.207	72.41	39.64	53.41	0.994	−48.4	1	0.366
1.75	2000	24.414	0.21	6.29	1.14	0.965	−76.2	2	0.366
1.5	500	3.418	2.13	1.21	1.60	0.993	−46.2	1	0.410
1.5	500	6.836	0.12	0.19	0.14	0.873	−89.8	2	0.410
1.5	1000	7.080	3.44	8.55	5.23	0.931	−25.6	1	0.425
1.5	1000	14.160	1.83	0.96	1.32	0.995	−85.9	2	0.425
1.5	1500	10.742	81.23	23.34	43.48	0.997	−49.1	1	0.430
1.5	1500	21.484	5.50	2.48	3.67	0.991	−100.7	2	0.430
1.5	2000	14.404	144.71	69.83	100.47	0.999	−42.3	1	0.432

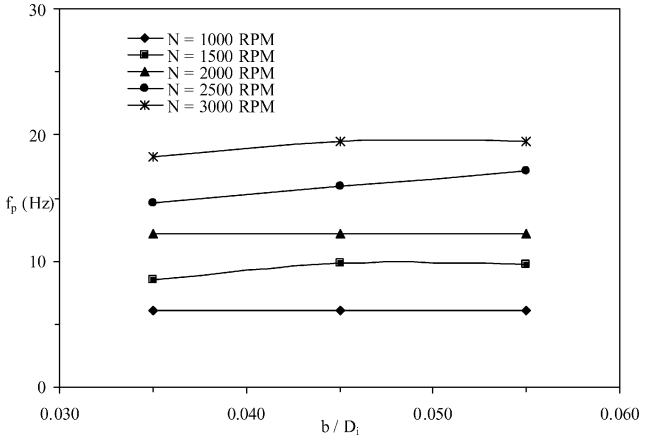

Fig. 9 Effects of diffuser width ratio on frequency of pressure fluctuations, $D_o/D_i = 1.5$.

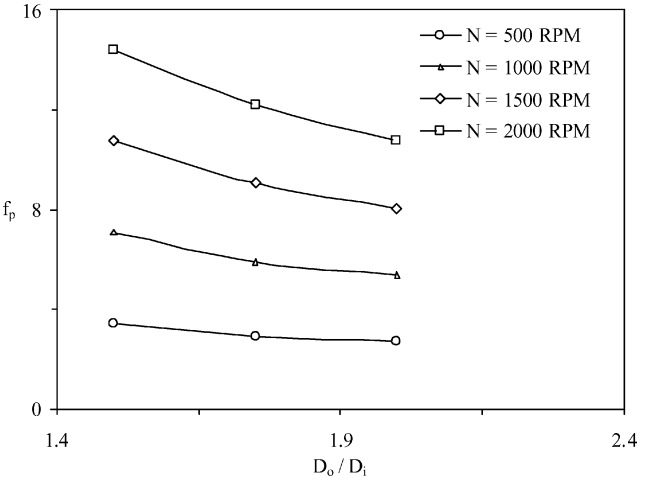

Fig. 10 Effect of diffuser diameter ratio on stall cell frequency at different rotor speeds.

fluctuation of the rotating stall cells increases slightly as the diffuser width was increased, although this trend is not very clear for $N < 2500$ rpm. Hence, it could be concluded that the diffuser width ratio has an insignificant effect on the subsynchronous frequency at which rotating stall features.

Diffuser Diameter Ratio

The effects of diffuser diameter ratio on stall characteristics are tabulated in Table 3. Table 3 shows the existence of a primary stall cell with one lobe and its second harmonic at all of the diffuser diameter ratios tested. The signal outputs from the pressure transducers are highly coherent, as shown in the φ column.

The effect of diffuser diameter ratio, on the frequency of pressure fluctuation, as a function of impeller rotational speed, is shown in Fig. 10. For all of the impeller speeds shown in Fig. 10, the frequency of pressure fluctuations decreases as the diffuser diameter ratio was increased. Note that the slope of the curves in Fig. 10 increases with increase in the impeller angular speed. In other words, for a fixed increase of 33.33% in the diffuser diameter ratio, the decrease in the frequency of pressure fluctuation increases with an increase in the impeller angular speed. For example, the frequency of pressure fluctuations f_p decreased by 21.43, 24.14, 25, and 25.42% for impeller angular speeds of 500, 1000, 1500, and 2000 rpm, respectively, when the diffuser diameter ratio was increased by 33.33%.

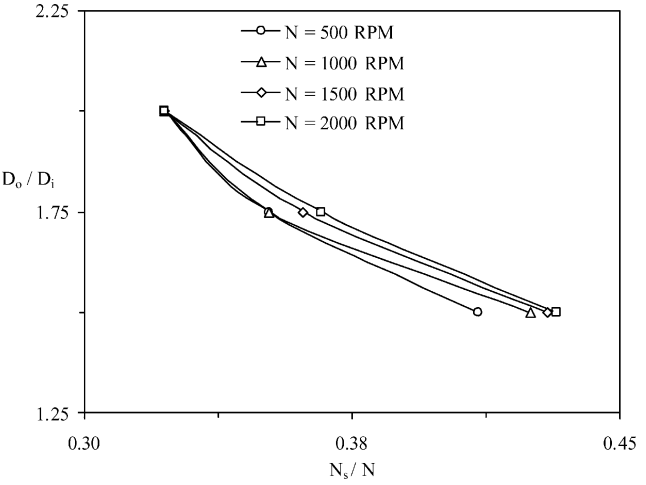

Fig. 11 Effect of diffuser diameter ratio of nondimensional frequency of rotating stall.

The effect of diffuser diameter ratio on the nondimensional speed of the stall cells is shown in Fig. 11. For all of the impeller angular speeds shown, the nondimensional speed of the stall cells increases as the diffuser diameter ratio was decreased. For example, a decrease of 12.5% in the diffuser diameter ratio (from $D_o/D_i = 2$ to 1.75) resulted in an increase of 13.6% in the nondimensional rotational speed of the one-lobe stall cell when the impeller was operated at $N = 2000$ rpm. The results in Ref. 16 showed similar strong dependence of the stall cell speed on the diffuser diameter ratio. For example, a decrease of 15.3% in the diffuser diameter ratio resulted in about 22.7% increase in the nondimensional speed of the single-lobe stall cell. Thus, it could be concluded that the nondimensional speed of stall cells is strongly dependent on the diffuser diameter ratio when compared to the effect of the diffuser width ratio.

Conclusions

The following conclusions could be drawn from the discussion.

1) Only one fundamental stall cell, featuring at a subsynchronous frequency of 13.4 Hz, was found with its harmonics. This stall cell frequency reduces to 12.2 Hz as the flow was reduced further, suggesting throughput influences stall frequency.

2) The performance of the blower, in terms of stability, is better with a smaller diffuser diameter, if all other geometric parameters are kept constant. Similarly, the stability of the blower increases as the diffuser width is increased, if all other geometric parameters are unchanged.

3) For a fixed diffuser width, the frequency of stall cells increased as the diffuser diameter ratio was decreased. There was no appreciable change in the propagating stall frequency when the diffuser width was altered.

4) The strength (CSD) of the rotating stall cell increases as the flow coefficient is reduced further from the critical flow coefficient. The strength of stall cells and stall cell frequencies are mostly independent of the diffuser width.

5) Diffuser diameter ratio has a significant effect on stall cell frequencies. Frequencies at which primary stall features decrease, with increasing diffuser diameter ratio.

6) The nondimensional speed of stall cells is strongly dependent on the diffuser diameter ratio and weakly dependent on the diffuser width ratio.

Acknowledgment

The author would like to acknowledge the support of King Fahd University of Petroleum and Minerals and Saudi Basic Industries Corporation in the preparation of this paper.

References

[1]Ishida, M., Sakaguchi, D., and Ueki, H., "Suppression of Rotating Stall by Wall Roughness Control in Vaneless Diffusers of Centrifugal Blowers," *Transactions of the ASME, Journal of Turbomachinery*, Jan. 2001, pp. 64–72.

[2]Watanabe, H., Konomi, S., and Ariga, I., "Transient Process of Rotating Stall in Radial Vaneless Diffusers," American Society of Mechanical Engineers, ASME Paper 94-GT-161, June 1994.

[3]Ohashi, H., and Shoji, H., "Lateral Fluid Forces on Whirling Centrifugal Impeller (2nd Report: Experiment in Vaneless Diffuser," *Transactions of the ASME, Journal of Fluids Engineering*, Vol. 109, No. 2, 1987, pp. 100–106.

[4]Fringe, P., and Van den Braembussche, R., "A Theoretical Model for Rotating Stall in the Vaneless Diffuser of a Centrifugal Compressor," *Journal of Engineering for Gas Turbines and Power*, Vol. 107, April 1985, pp. 507–513.

[5]Abdelhamid, A. N., "Effect of Vaneless Diffuser Geometry on Flow Instability in Centrifugal Compression Systems," *Canadian Aeronautics and Space Journal*, Vol. 29, Sept. 1983, pp. 259–288.

[6]Rodgers, C., and Mnew, H., "Experiments with a Model Free Rotating Vaneless Diffuser," American Society of Mechanical Engineers, ASME Paper 74-GT-58, March 1974.

[7]Abdelhamid, A. N., "Analysis of Rotating Stall in Vaneless Diffusers Compressors," *Canadian Aeronautical and Space Journal*, Vol. 26, No. 2, 1980, pp. 118–128.

[8]Abidogun, K. B., "An Experimental Investigation of Stall Characteristics in Vaneless Diffusers," Ph.D. Dissertation, Mechanical Engineering Dept., King Fahd Univ. of Petroleum and Minerals, Dhahran, Saudi Arabia, May 2000.

[9]Abidogun, K. B., "Rotating Stall in the Radial Vaneless Diffuser of a Centrifugal Blower," *Proceedings of the Workshop on Energy Conservation in Industrial Applications*, King Fahd Univ. of Petroleum and Minerals, Dhahran, Saudi Arabia, 2000, pp. 413–421.

[10]Otugen, M. V., So, R. M. C., and Hwang, B. C., "Diffuser Stall and Rotating Zones of Separated Boundary Layer," *Experiments in Fluids*, Vol. 6, No. 8, 1988, pp. 521–533.

[11]Abdelhamid, A. N., "Control of Self Excited Flow Oscillations in Vaneless Diffuser of Centrifugal Compressor Systems," *Canadian Aeronautics and Space Journal*, Vol. 29, Dec. 1983, pp. 336–345.

[12]Kinoshita, Y., and Senoo, Y., "Rotating Stall Induced in Vaneless Diffuser of Very Low Specific Speed Centrifugal Blowers," *Journal of Engineering for Gas Turbine and Power*, Vol. 107, April 1985, pp. 514–521.

[13]Jansen, W., "Rotating Stall in a Radial Vaneless Diffuser," *Journal of Basic Engineering*, Vol. 86, Dec. 1964, pp. 750–758.

[14]Senoo, Y., and Kinoshita, Y., "Influence of inlet Flow Conditions and Geometries of Centrifugal Vaneless Diffusers on Critical Flow Angle for Reverse Flow," *Journal of Fluids Engineering*, Vol. 99, March 1977, pp. 98–103.

[15]Cumpsty, N. A., *Compressor Aerodynamics*, Addison Wesley Longman, Harlow, England, U.K., 1989, Chap. 7, p. 279.

[16]Abdelhamid, A. N., and Bertrand, J., "Distinction Between two types of Self Excited Gas Oscillations in Vaneless Radial Diffusers," *Canadian Aeronautics and Space Journal*, Vol. 26, No. 2, 1980, pp. 105–117.

[17]Mizuki, S., and Oosawa, Y., "Unsteady Flow Within Centrifugal Compressor Channels Under Rotating Stall and Surge," *Transactions of the ASME*, Vol. 114, April 1992, pp. 312–320.